

Temperature dependence of ultracold neutron loss rates

E. Korobkina and R. Golub

Hahn-Meitner Institute, Glienickerstrasse 100, 14109 Berlin, Germany

J. Butterworth and P. Geltenbort

Institut Laue-Langevin, Boîte Postale 156, 38042 Grenoble Cedex 9, France

S. Arzumanov

RRC Kurchatov Institute, Kurchatov Square 1, 123182 Moscow, Russia

(Received 22 January 2004; published 15 July 2004)

The discrepancy between measured ultracold neutron (UCN) loss rates and those predicted from pure materials has been the subject of study for over 30 years. Nevertheless, the data about UCN upscattering to the meV range, which is the main cause of UCN losses over a wide temperature range, are still contradictory and rather poor, especially at low temperatures. The low-temperature behavior of the upscattering loss rate is crucial for distinguishing between different models of this process. Here we report a study of UCN upscattering in a well controlled sample environment (ultrahigh vacuum) and at temperatures down to 4 K. We studied UCN interaction with chemically bound hydrogen. In our data interpretation we used data for the surface chemical content of our storage bottle that were measured with elastic recoil detection analysis as well as phonon data from neutron inelastic scattering. The complex analysis allows us to rule out the model of sub-barrier upscattering inside the bulk material and demonstrate a good agreement between experimental data and a “ $1/v$ ” model consisting of a thin hydrogenous film or clusters with low Fermi potential. The phonon spectrum of ice can easily explain the observed low-temperature losses. Finally, we discuss possible application of UCN upscattering to condensed matter study.

DOI: 10.1103/PhysRevB.70.035409

PACS number(s): 68.49.-h, 78.70.Nx, 68.47.-b

I. INTRODUCTION

Ultracold neutrons (UCN's) play an increasingly important role in experiments studying the fundamental properties of the neutron [neutron lifetime, neutron electric dipole moment (EDM), β -decay asymmetries]. The unique feature of UCN's, their ability to be confined for long times (tens of minutes) in material and magnetic bottles offers the possibility of a significant increase in accuracy over more classical methods for many experiments. There are several projects including high-density UCN sources and fundamental physics experiments that are currently in operation at or being designed for operating at low temperatures¹⁻⁶ that are favorable for both storage and production of UCN's. In the present publication we discuss only material bottles, where UCN's are confined by the nuclear Fermi pseudopotential.

The limitations on the storage time in material traps come from the neutron β -decay lifetime and interaction with the surface. The latter causes the ultracold neutrons to escape from the confinement volume. Depending upon the material, temperature, and surface state of the trap, either nuclear absorption or energy gain could be the dominant escape channel. Whereas the capture could be minimized by proper choice of a weak absorbing material, the suppression (by low temperatures) of the upscattering to the level required for the direct measurement of the neutron lifetime with uncertainty below 1 s is still problematic. Details of the upscattering process have been and are the subject of some controversy, with a range of models proposed to explain the observed losses.⁷⁻⁹ Some observers even argue that the measured losses are too large to be explained by conventional

physics.¹⁰ On the other hand, it was the detection of the upscattered neutrons that allowed the achievement of the lowest level of systematic uncertainty (0.4 s) in the neutron lifetime.¹¹ Thus progress in understanding UCN interactions with surfaces is both interesting and important for particle physics, and further progress in this direction could possibly offer an additional technique for studying surfaces.

Recent years have been very productive in getting deeper insights into UCN interaction with matter. The UCN absorption was studied with prompt (n, γ) analysis and an unpredicted effect of the selective loss enhancement due to clusters was discovered.^{12,13} Quasielastic scattering with neV energy transfer was recently observed and gave rise to quite intensive theoretical and experimental studies.¹⁴⁻¹⁸ At present it seems to be clear that “small heating” affects only the UCN's storage on fluoropolymer oil down to a certain temperature (and is undoubtedly due to scattering on surface waves¹⁹), while for solids it is negligible except for one case of some special treatment, not yet understood.²⁰ Thus the main effect on solids with a small neutron absorption, for instance Be, remains the upscattering to the meV range. It was intensively studied experimentally in the 1970s and 1980s when trying to explain the loss probability at the level of 10^{-3} – 10^{-4} at room temperature, but the main problem, that of finding experimentally the correct model to calculate the UCN upscattering, has not been solved yet. For the neutron lifetime experiments a proper model is crucial for the technique where the calculated effective frequency of collision is involved.²¹ After over 30 years of study, the only well established fact about the UCN losses due to inelastic upscattering is the conclusion that it is caused by hydrogen con-

tamination. The main evidence is the observation of the temperature dependence of the UCN loss rate and the linear correlation between the probability of UCN inelastic scattering and the amount of hydrogen.^{22,23} Indirect but important evidence was detection of hydrogen in 50 Å surface layers of Cu and carbon in the range of (50–30)% after applying the usual surface treatment technique used in UCN storage bottles.²⁴ Unfortunately, the low-temperature upscattering has never been adequately studied, while it is crucial for distinguishing various models of the upscattering process.

Indeed, the experimental data are rather poor, especially below 77 K. There has been only one study of the temperature dependence, which was carried out at the Institut Laue-Langevin (ILL), Grenoble, France, in the temperature range from 6.5 K up to 300 K;²⁵ then there are data from neutron lifetime measurements by means of a Gravitrap conducted at Petersburg Nuclear Physics Institute (PNPI), Gatchina, Russia, down to 13.5 K.²⁶ The results of both at first glance seem to give evidence of excess losses at low temperature and give rise to the idea of a low-temperature “anomaly” in UCN interaction with solid matter. Nevertheless, a more careful analysis of the experimental conditions and data evaluation points more likely toward technical problems. One of the issues was the quality of the Be coating. Our test of Be, double Be, and stainless steel coatings on Al foils and Si wafers directly proved that this is really the case.²⁷ The typical value of UCN transmission through Be coatings on unpolished Al foil was in the range $\approx 10^{-4}$ while the best result was for the silicon wafer, 0.7×10^{-4} . The energy dependency of the transmission shows that it arises due to pinholes in the Be coating. When a trap is filled with a Maxwellian-like spectrum, the presence of pinholes gives rise to a dramatic difference between the loss rates for neutrons with energy below and above the Fermi potential of the substrate. Due to the geometry of the storage trap (long, narrow cylinder, average frequency of collisions 80 s^{-1}) the ILL experiment was very sensitive to this effect. Using a detailed description of the experiment, one can easily reconstruct the storage curves numerically and see that taking into account transmission $\approx 0.5 \times 10^{-4}$ (for an electropolished tube), the correct value of the Be absorption cross section, the loss rate due to hydrogen absorption $\approx 0.005/15 = 0.3 \times 10^{-3}$, and the valve loss rate $\approx 1 \times 10^{-3}$ leaves no place for the anomaly that was observed in the Gatchina experiment (which would lead to a loss rate $\approx 2.4 \times 10^{-3}$). This reconstruction is in perfect agreement with the UCN storage curve observed earlier in the same apparatus when it was used as an UCN superthermal source²⁸ without a Be coating. The pinhole effect makes it difficult to use ILL data for theoretical analysis.

In the Gatchina experiment the high-energy neutrons were specially cleaned from the UCN spectrum, but still the energy dependence of losses looks more like that on Al rather than on Be. In Ref. 29, the authors explained it by losses on the outer surfaces in the course of emptying so it seems that the pinholes were not a big issue, but the pumping was. Indeed, contrary to the ILL experiment, where 4 K and 77 K were measured with the storage bottle sealed to prevent cryopumping, the storage volume in the Gatchina experiment was continuously pumped with a diffusion pump through a 77 K trap. The latter is not efficient at $T \leq 77 \text{ K}$. While a

diffusion pump provides a stable vacuum it unavoidably contaminates the surface. The significant improvement of the storage time at 4 K after oxygen spraying (which works as a cryopump) looks like a good confirmation of this origin of the largest part of anomaly. The quality of the pumping was always an issue in the old experiments. Therefore the data on Be from both experiments should be used with great care.

Recently, a more detailed study of the temperature dependence on several materials was performed but only down to 77 K. The conclusion of the study on the Be foil was that at 77 K there is still a loss probability equal to 2.5×10^{-5} per collision.³⁰ The theoretical model (hydrogen oscillation with phonon frequency of the Be spectrum but with a proton as a scatterer), gives a reasonable value for the cross section at 300 K, but was not able to reproduce the temperature dependence below 300 K. Calculating the loss probability per collision for the room temperature, the authors obtained agreement only when taking 96% of the hydrogen concentration in the surface layer, which seems to be unreasonable. A recent study of pyrolytic graphite again shows a considerable loss rate at 77 K.³¹ The authors assumed that the origin could be related to the binding conditions of the hydrogen. The recent results of the neutron lifetime measurement on Fomblin oil clearly addressed the issue of the low-temperature loss to upscattering,³² which was found to be several times higher than expected.³³

Roughly speaking, it is clear that UCN's are upscattered mostly by hydrogen, but it is not clear how and on what kind of hydrogen — chemically, tightly or weakly bound to the bulk material, or in a two-dimensional gas, or something else. In addition there has not been a rigorous theoretical study of UCN upscattering. Model calculations of UCN upscattering exist only on a rather naive estimations level. The earlier theoretical works^{34,35} were trying to get agreement at the level of loss probabilities $10^{-3} - 10^{-4}$ per collision, while the present experiment are working in the range $\approx 10^{-5} - 10^{-6}$. The models used for data interpretation seem to be incomplete and questionable.

Motivated by the interest in finding out what is the real low-temperature dependence of UCN losses and in finding a quantitative model based on the available data for the surface and solid state physics, we commissioned an ultrahigh-vacuum cryostat, which allows us to study the UCN loss rate in a well controlled environment over a wide temperature range. As a sample surface to begin with we used copper, which is well studied in surface physics, neutron scattering, and UCN storage at room temperature. The phonon spectrum and mass of the copper are very different from those of Be. The first experiment was performed on the PF2 instrument, test beam position at the Institut Laue-Langevin.

II. DESCRIPTION OF THE EXPERIMENT

Since UCN's are interacting with a thin surface layer (approximately 100 Å) the main issue in an experiment is to prevent any change of the surface state during cooling or heating. When cooling down to 20 K the absorption of residual hydrogen may occur. When heating up one should take care about possible adsorption from hotter outgassing

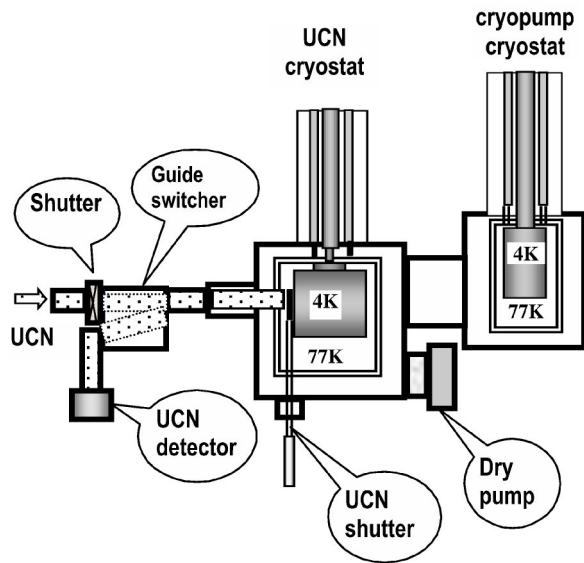


FIG. 1. Experimental layout.

surfaces. In the ILL experiment this problem was solved by separating vacuums and sealing the storage volume after outgassing under heating, while in the Gatchina study the storage bottle was enclosed in an outer housing that was not sealed but continuously pumped through a 77 K trap. It was the outer housing that was heated and cooled. Therefore, in principle, one cannot exclude that excess (relative to theory) losses in the Gatchina experiment below 77 K may partly originate from both the heating procedure, when impurities come from the hot housing, and cooling, when owing to the long duration of the measurement some residual gas gets adsorbed through the pumping line. Moreover, as was recently observed,²⁰ heating above 200°C may produce some phase or destructive changes on the surface, and the effect of small UCN heating can be enhanced by several orders of magnitude. In our study we tried to take care and keep the environment of our surface under control.

Our experimental layout is shown in Fig. 1. We do not use a separate vacuum but the whole apparatus was constructed to ultrahigh-vacuum standards, i.e., only metal seals were used (CF flanges with Cu gaskets and wire sealing with annealed Al, In, and Au); no plastic parts, only metal and ceramic; dry pump system (turbomolecular pump and scroll forpump, Varian). The cryostat has five free outlets with CF-100 flanges around the main vacuum housing. One was used to connect a neutron guide through 100 μm Al foil. The turbomolecular pump was also mounted directly on another CF-100 outlet. In addition we have another cryostat working as a cryopump that is connected through an outlet 20 cm long, 25 cm in diameter to the main housing. Both cryostats are of the same construction (Oxford Instruments, UHV modification), but the UCN cryostat is attached to the UCN bottle and the cryopump cryostat is connected to large-area Cu baffles connected to both liquid nitrogen (LN) and liquid helium (LHe) baths. Thus we have very high-efficiency pumping system.

Both heating and cooling were performed by direct contact of the storage bottle with a central part of the cryostat,

which contained either a heating resistor or liquid nitrogen or liquid helium. Thus during heating the storage bottle was the hottest part of the apparatus whereas during cooling and at room temperature the coolest part was the cryopump filled with LN and LHe.

The UCN storage bottle was surrounded by an additional 4 K thermal shield made from Cu, attached to the top of the bottle, and several layers of Al foil. One platinum resistor Pt100 (at the bottom) and two carbon resistors (bottom and top) were used to measure the temperature. The temperature of the bottom of the 77 K shield was also measured by a Pt100 resistor. A third carbon resistor was mounted on the sliding UCN shutter. Both the UCN bottle and 77 K shield were made from unpolished oxygen-free high-conductivity copper. The UCN bottle was a horizontal cylinder of 18 cm inner diameter and 19 cm long. UCN entered the bottle through a 5 cm diameter opening in one of the vertical end flanges. A sliding shutter was used to close the entrance hole. The opening in the 77 K shield has a 10 μm Al window to prevent 300 K irradiation from the inner neutron guide from reaching the 4 K parts. The 300 K vacuum housing was attached to the PF2 test beam through an adapter flange with a 100 μm vacuum tight Al window. The neutron detector was attached to the guide switcher. The distance between the UCN bottle and UCN detector was about 1.5 m. It took us 25 min to cool the UCN bottle from 77 K down to 4 K. We had to refill the LHe bath twice per day. The LN filling was arranged to be automatic. The best vacuum during measurement was at the lowest limit of our vacuum gauge, i.e., $\leq 10^{-9}$ mbar. We performed two runs for two different states of the Cu surface. Prior to the first run the bottle was ultrasound cleaned in distilled water and before the second run it underwent deuteration. Before deuteration the surface of the bottle was etched with 5% nitric acid and washed with acetone and ethanol. Deuteration was performed by heating in a vacuum oven up to 240°C and slow cooling down to room temperature in a vapor of D₂O at approximately 10 mbar pressure for 24 h.

The sequence of data taking for both surface states was as follows: (1) 300 K, room temperature, initial state; (2) 450 K, steady state after “mild” outgassing; this temperature is sufficient to remove a water film but hopefully does not affect the surface; (3) 300 K, slow cooling down, cryogenic pump is filled with LN and LN; (4) 77 K, UCN cryostat is filled with LN, cryogenic pump is filled with LHe and LN; (5) 4 K, UCN cryostat is filled with LHe and LN, cryogenic pump is filled with LHe and LN; (6) 77 K, UCN cryostat is filled with LN and LN, cryogenic pump is filled with LHe and LN; (7) 170 K, UCN cryostat 4 K bath is empty, 77 K bath is filled with LN, cryogenic pump is filled with LHe and LN.

In the second run steps 5 and 6 were repeated twice more to check the reliability of the data, while in the first run step 7 was skipped. In the first run we were adjusting our intervals for filling, cleaning, storing, and emptying the bottle while the cryostat was cooling down to 77 K. Therefore only the low-temperature data of run 1 (77 K and 4 K points, see below) may be used for physical conclusions.

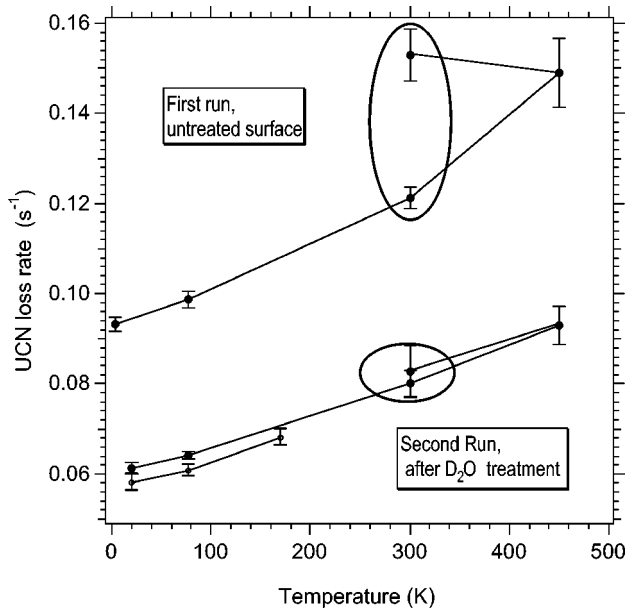


FIG. 2. Raw data for two different surface treatments prior to the measurement with UCN's: the upper curve, run 1, the surface was washed in the ultrasonic bath with distilled water; the lower two curves run 2, the surface was heated in D_2O vapor in the vacuum oven. The ovals show the comparison of 300 K data before and after heating of the storage bottle inside the UHV cryostat.

III. EXPERIMENTAL RESULTS

The technical test of the UHV cryostat was successful. The vacuum conditions during data taking were less than 10^{-8} mbar in the first and less than 10^{-9} mbar in the second run. We do not see any temperature hysteresis. We could easily cool down the storage bottle to 4 K. The only trouble was that the shutter on the UCN bottle was not sealing the storage volume properly, giving rise to additional losses. Since this offset in the loss rate is temperature independent, it did not affect the temperature dependence study. In run 2 the adjustment of the UCN shutter was improved, giving better storage time. The radiation shield of the UCN bottle was simplified to improve the pumping speed. A later test revealed that it was a bad thermal contact, giving ≈ 20 K offset to a higher value. Therefore, we are sure that the temperature at the bottom was at least 10 K while the top was at 4 K.

The raw data for the temperature dependence of the loss rate for both hydrogenated and deuterated surfaces are shown in Fig. 2. The upper curve corresponds to the first run, when the storage time was shorter and the surface contained more hydrogen. The two lowest curves were measured after deuteration of the surface and improvement of the UCN shutter. Nevertheless, in the second run during first warming up from 4 K up to 77 K the shutter again was adjusted, giving rise to a slightly better storage time (the lowest short curve). To check the stability we repeated the cooling down and warming up between 4 K and 77 K twice. The results were indistinguishable from each other. This can be considered evidence that we did not have any significant adsorption at the lowest temperatures and our data can be used for a theoretic

cal interpretation. Thus the average values are presented on the lowest curve of Fig. 2 to decrease the statistical uncertainties.

Clearly, the statistics could be improved. Nevertheless, we may already conclude that data from both run 1 and run 2 demonstrate a well pronounced temperature dependence below 77 K, with differences only in the amount of hydrogen. Another important observation is that our annealing procedure in D_2O vapor made the Cu surface hydrophobic. Indeed, after deuteration the bottle was exposed to the high-humidity air of the experimental hall overnight, but the loss rates on the nonheated and heated deuterated surfaces are practically the same in contrast to the case of the undeuterated surface (run 1). Therefore, the temperature dependence of the second run is free from the contribution of physisorbed contamination and may be related to chemically bound hydrogen.

Several months after the measurement with UCN's was done, the chemical content of the copper surface was studied using elastic recoil detection analysis (ERDA) at ISL, HMI. It turns out that the hydrogen content in the bulk ($> 2 \mu\text{m}$) is 0.1% while in the surface layer (7.2×10^{17} at./ cm^2 at., $\approx 100 \text{ \AA}$) it was found to be 8% (5.8×10^{16} at./ cm^2). The rest was Cu(55%), C(10%), O(25%), with small traces of contamination by Cl, S and Na. Deuterium was found in the amount of 0.6×10^{15} at./ cm^2 and was probably not directly on the surface. The latter conclusion is approximate because the ERDA technique could not distinguish between deepness and roughness. Our surface was never polished and was visually rough and oxidized after deuteration. The sample was annealed in the vacuum oven at 200°C before measurement. Nevertheless, an accumulation of contamination from the atmosphere (20–30%) could also affect the results. Therefore, we should consider the observed amount of hydrogen as an upper limit.

IV. DATA INTERPRETATION

For the discussion below we consider only the temperature-dependent part of the loss rate $1/\tau(T) = 1/\tau_{\text{expt}}(T) - 1/\tau_{\text{expt}}(10 \text{ K})$. To improve the statistics both curves of run 2 were averaged together. The upper limit on the amount of hydrogen in the top layer of 8% allowed two models to be considered. One is a dilute solution of hydrogen in copper, while the other is a hydrogenated film or film clusters on the Cu substrate. In both cases the shape of the temperature dependence arises from the temperature behavior of the inelastic upscattering cross section, while the actual loss rate depends as well on the ratio between the Fermi potential and neutron energy.

If the surface is a compound of several elements, the total loss rate is the sum of the partial losses. Since for C, O, D, and Cu both coherent and incoherent upscattering cross sections for the temperature range 500–4 K are rather small, the observed value of the losses should be attributed to incoherent upscattering on hydrogen. Indeed, in the (n, γ) study^{36,37} a linear correlation between the UCN absorption rate on hydrogen, μ_{cap} , and the upscattering rate μ_{ie} was observed. μ_{cap} is proportional to the hydrogen concentration that was

changed by annealing of the sample. Thus the correlation between μ_{cap} and μ_{ie} is direct evidence of the hydrogen origin of the UCN upscattering. Moreover, from the linear fit it was found that

$$\mu_{ie} \approx 17\mu_{cap}. \quad (1)$$

Since both rates are proportional to the cross sections, the formula (1) allows us to estimate the absolute value of the neutron upscattering on the Cu surface, $\sigma_{ie}(\text{Cu}) \approx 17\sigma_{cap}(\text{H}) = 5.6\text{b}$ per proton for thermal neutrons. It is an average value for the sample coated with water film and annealed at 750°C . For the samples annealed with an intermediate step the coefficient of the proportionality was changed to 12–15 for all studied samples. This implies that $\sigma_{ie} \approx (12\text{--}15)\sigma_{cap}(\text{H}) = 4\text{--}5\text{b}$ per proton. This value might certainly be related to a surface without physisorbed water.

We start from a model of a dilute solution which means a subbarrier (the UCN energy is below the potential barrier produced by the bulk material) UCN interaction with hydrogen tightly bound to the heavy copper atoms. To calculate the upscattering cross section $\sigma_{ie}(\text{H}, \text{Cu})$ we have used a one-phonon approximation, the general formula of which can be written as follows:

$$\sigma_{up}(T) = 4\pi b^2 \int e^{-2W(T)} G(\omega) n(\omega, T) \sqrt{\frac{\omega}{E_0}} d\omega, \quad (2)$$

where E_0 is the energy of the neutron, $n(\omega, T) = 1/[\exp(\omega/T) - 1]$ is the occupation factor, the integration is taken over the entire frequency range, $W(T)$ is the Debye-Waller (DW) factor

$$2W(T) = \omega \int_0^{\omega_{\max}} \frac{G(\omega')}{\omega'} \coth \frac{\omega'}{2T} d\omega', \quad (3)$$

and the function $G(\omega)$ is a generalized density of vibrational states (GDVS) of hydrogen. Formulas (2) and (3) are derived from the standard expression for the double differential cross section and DW factor (see, for instance, Ref. 38) taking into account the angular isotropy of the upscattered neutrons and the fact that in the case of UCN the initial energy $E_i \approx 0$. Thus both momentum Q and energy transfer ε are equal to the momentum and energy of the annihilated phonon, $Q = q_i - q_f \approx q_f$, $\tilde{\varepsilon} = E_i - E_f \approx E_f = \omega = Q^2/2m$, where m is a neutron mass. For the discussion below we have emphasized terms dependent on T .

It is known that hydrogen tightly bound to a metal lattice undergoes two types of vibrations: acoustical, in the energy range up to $\approx 40\text{--}60$ meV, and optical with higher energies \approx above 100 meV. In the lattice branch hydrogen vibrates with the amplitude of the metal atoms, i.e., $G(\omega) \propto m/M$ and the mass in the denominator must be taken equal to the mass of copper, while in the optical branch pure hydrogen vibrations occur and $M=1$. For the heavy metals this leads to significant suppression of the scattering from the acoustical vibrations compared with the optical ones. Nevertheless, as we see below, the relative contribution of both branches to the neutron cross section depends strongly upon temperature.

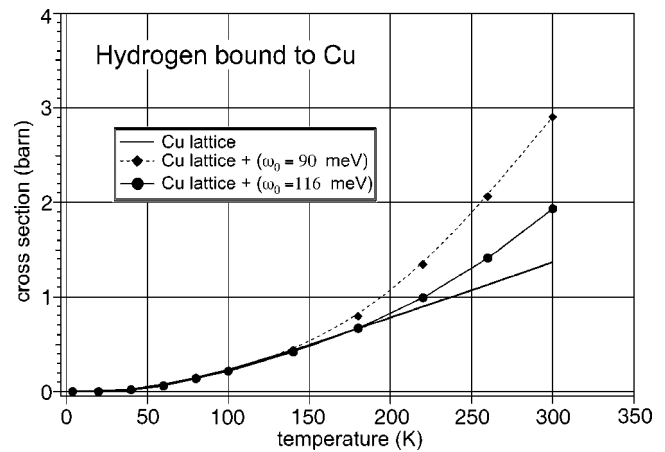


FIG. 3. The upscattering cross sections of UCN calculated in the one-phonon approximation for H bound to Cu: the bottom curve takes into account only the lattice vibrations; the two top curves show the effect of the addition of the optical branches $\omega_{opt}=116$ and 90 meV.

The shape of the acoustical part mirrors the shape of the phonon spectrum of the lattice and the optical part could be modeled by an Einstein oscillator. Thus in a very simple way the GDVS of hydrogen in Cu could be reconstructed as follows:

$$G(\omega) = \begin{cases} \mu g_{\text{Cu}}(\omega), & \omega < 40 \text{ meV}, \\ \delta(\omega - \omega_{opt}), & \omega \geq 40 \text{ meV}, \end{cases} \quad (4)$$

where $\mu = m/M_{\text{Cu}} = 1/65$, ω_{opt} is the optical frequency, and we assume an equal number of acoustical and optical branches. The normalization is chosen to be for calculating a cross section per each nucleus. The phonon spectrum of the copper lattice was calculated in Ref. 39 based on experimentally measured force constants. The value of ω_{opt} was estimated from the experimental study of CuPdH to be ≈ 116 meV.⁴⁰

In Fig. 3 we plot calculated cross sections for UCN upscattering on H-Cu. The lowest curve shows the contribution of the lattice part, while the other two were calculated using Eq. (4) with $\omega_{opt}=116$ and 90 meV to investigate the effect of different optical vibrations.

As we can see, the contribution of the lattice part dominates the entire temperature range. Nevertheless, the optical branch plays an important role by changing a linearlike shape to a power law and increasing the absolute value of the cross section at $T > 200$ K. As a result, in contrast to the experimental value of the ratio $\eta_{\text{expt}}(300)/\eta_{\text{expt}}(77) \approx 7$, the calculated value $\sigma_{ie}(300)/\sigma_{ie}(77) \approx 14$ if $\omega_{opt}=116$ meV or even larger (≈ 22) for smaller $\omega_{opt}=90$ meV, while for the lattice part itself the ratio ≈ 10 . Thus this model cannot reproduce the shape of the experimental T dependence. It also fails to reproduce the (n, γ) estimation of $\sigma_{ie}(300) = 4\text{--}5.6$ b.

Now let us discuss the probability of UCN subbarrier upscattering per collision, η_{ie} . The theoretical temperature dependent probability per collision, $\eta(T)$, for sub-barrier UCN

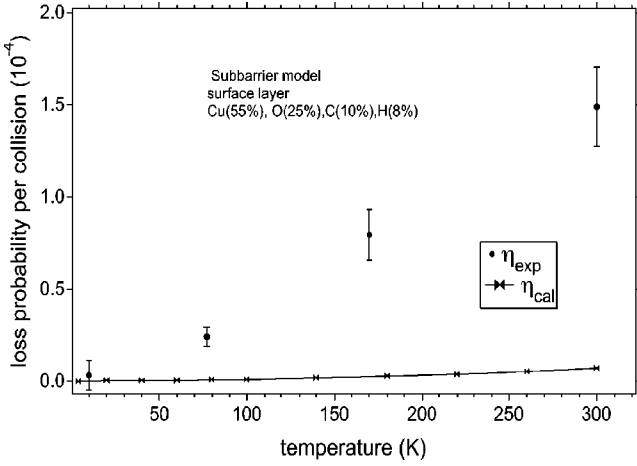


FIG. 4. Upscattering probabilities per collision for the subbarrier model: $\eta_{\text{exp}}(T)$ is derived from experiment and $\eta_{\text{cal}}(T)$ is calculated using $\sigma_{ie}(T)$ for hydrogen bound to Cu.

losses can be calculated from $\sigma_{ie}(T)$ using the optical potential approximation in the following way:

$$\eta(T) = \frac{\sum_i c_i \sigma_{up}^i(T)}{2\lambda \sum_l c_l b_l} \approx c_H \frac{\sigma_{up}^H(T)}{2\lambda \langle b \rangle}, \quad (5)$$

where $\sigma_{up}^i(T)$ is the partial upscattering cross section for the neutron wavelength λ ; b_i is the scattering length and c_i is the partial concentration of the i nucleus. We took into account that the denominator describes the average scattering length of the surface layer, $\langle b \rangle = 6.09$, calculated for a homogeneous mixture of Cu(55%), O(22%), C(10%), and H(8%). The experimental values were derived from the raw data in the usual way,

$$\eta_{\text{H,Cu}} = \frac{1}{\tau \langle \nu f \rangle}, \quad (6)$$

where τ is the storage time and $\langle \nu f \rangle$ is the mean effective frequency of collision. The latter term $\langle \nu f \rangle$ was calculated to be approximately $\langle \nu f \rangle = 65 \text{ s}^{-1}$ using the mean UCN velocity averaged over the energy range from 50 neV (lower energy cut off by Al foil) up to 165 neV (higher energy cut off by Cu walls) and the geometrical area of the bottle. The surface area of a storage bottle depends on the surface roughness. Thus, the absolute values of both $\langle \nu f \rangle$ and $\eta_{\text{H,Cu}}$ are correct only within a factor. Since our bottle had an unpolished surface, we include an additional factor of 2 to account for the roughness which does not affect the temperature dependence itself.

The experimental probability derived from the data of run 2 is shown in Fig. 4 together with the Cu-H model calculations. It is clear that the loss probability $\eta_{\text{cal}}(T)$ calculated using formula (1) with 8% concentration of hydrogen is an order of magnitude below experimental values. Thus this

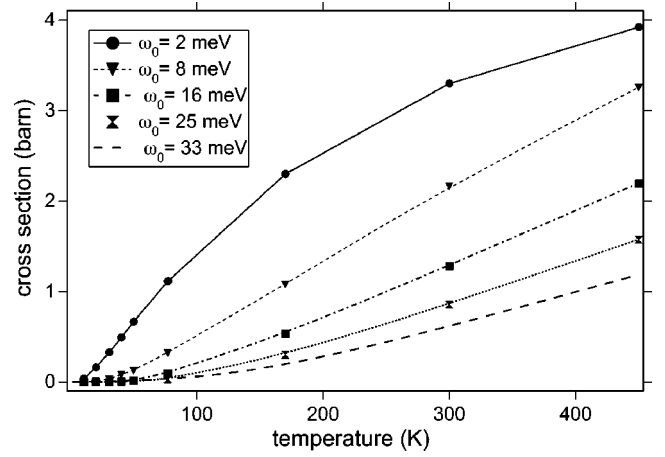


FIG. 5. Temperature dependence of the upscattering cross section calculated for harmonic oscillators with frequencies 2, 8, 16, 25, and 33 meV and mass ratio $\mu = 1/7$.

model can explain neither the shape of the temperature dependence, nor the amplitude of the UCN upscattering probability per collision.

To understand what frequencies in the spectrum of vibrations could reproduce the low-temperature part, we studied the general behavior of the upscattering cross sections. We chose an exact solution of the single harmonic oscillator in the form of sums as was first derived by Weinstock.⁴¹ The reason is that the multiphonon contribution can be neglected only for heavy scatterers with $m/M \ll 1$ and low temperatures $T < \omega_0$. That was the case when we considered the Cu-H model. Now we are investigating a wide temperature and mass range, where a single-phonon approximation simply does not work because its cross section approaches zero at temperatures $T > \omega_0$.

In this model we have sums over all possible transitions from state l to n with the energy and momentum transfers

$$\begin{aligned} \varepsilon = E_i - E_f \approx E_f &= (l - n)\omega_0 = Q^2/2m, \\ Q^2 &= 2m\varepsilon = 2m\omega_0(l - n). \end{aligned} \quad (7)$$

The upscattering cross section of UCN's could then be written as

$$\begin{aligned} \sigma_{up}(T) &= \sigma_{inc} \mu \sqrt{\frac{\omega_0}{E_{th}}} (1 - e^{-\omega_0/T}) \sum_{n=1}^{\infty} e^{-n\omega_0/T} (n!) \\ &\times \sum_{l=0}^{n-1} (\sqrt{n-l})! e^{-(n-l)\mu} [\mu(n-l)]^{(n-l)} \\ &\times \sum_{k=0}^l \frac{[-(n-l)\mu]^l}{k! (l-k)(n-l+k)}, \end{aligned} \quad (8)$$

where $\mu = m/M$, M is the mass of the oscillator, the incoherent cross section $\sigma_{inc} = 4\pi b_{inc}^2$, and we took into account that $\xi^2 Q^2 = Q^2/M\omega_0 = 2\mu(n-l)$, where ξ is the amplitude of the zero-point oscillation.

The results of our calculations are shown in Fig. 5. It is easy to see that to explain the shape of the low-temperature

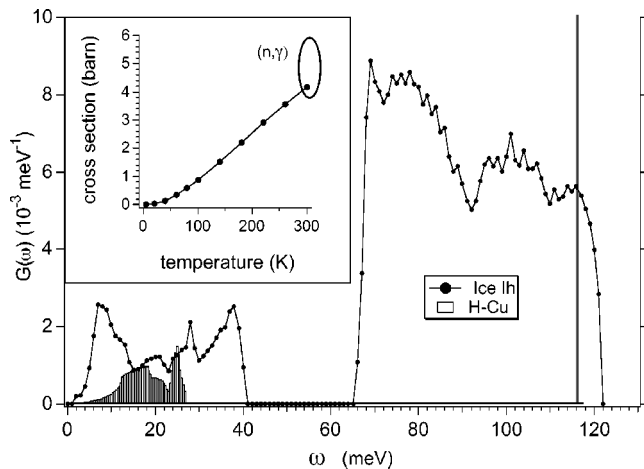


FIG. 6. Generalized density of states $G(\omega)$ for Cu(calculated) and ice *Ih* [from inelastic nuclear scattering data (Ref. 43)]. The inset shows $\sigma_{ie}(T)$ calculated using $G(\omega)$ of ice. The oval shows the range of $\sigma_{ie}(300)$ estimated from (n, γ) study.

part we need rather low oscillation frequencies below 10 meV. Moreover, the peak should be strong enough to give a contribution to the cross section, which is comparable with the higher frequencies. Otherwise switching on of the higher-energy branches will break the almost linear increase as the optical branch does in the Cu-H model. Such spectra are rather unusual for metal hydrides but typical for the intermolecular vibrations of molecules weakly bound to a crystal. We use $m/M=1/7$ to show that this value gives reasonable cross section values for a single oscillator. In reality it could be either carbon or/and oxygen always found in the top layer.

Thus, we naturally arrive at another, more realistic model of the UCN upscattering on the surface, that is, neutrons upscattered by a hydrogenated film or surface clusters with Fermi potential V_F close to zero. The UCN loss rate will obey a $1/v$ law and even a small amount of hydrogen could imply a significant upscattering rate. A similar situation was observed in stainless steel with UCN capture by Ti nuclei. 1% of Ti gave rise to the same capture rate as 50% of Fe due to the presence of clusters with $V_F=36$ neV compared to the average $V_F=185$ neV of the stainless steel.^{13,42}

Light hydrogenated molecules always present on the surface include, for instance, water. It turns out that the generalized density of states $G_{ice}(\omega)$ of ice indeed has a strong low-energy band with a peak at 7 meV.⁴³ To calculate the cross section we still could use formula (3), neglecting the multiphonon contribution that is about a few percent at 300 K.⁴⁴ Both the generalized vibrational density of state $G_{ice}(\omega)$ and $\sigma_{ie}(T)$ are shown in Fig. 6. The temperature dependence looks linear and $\sigma_{ie}(300)=4$ b. This value is in a good agreement with the (n, γ) estimation and the shape of the low-temperature part is in good agreement with the experimental data.

Now let us estimate the loss probability using the simplest model of a monoenergetic neutron interacting with a film $V_F^f < E_{UCN}$ and on a substrate with $V_F^s > E_{UCN}$. As was shown above, the temperature-dependent contribution from H-Cu

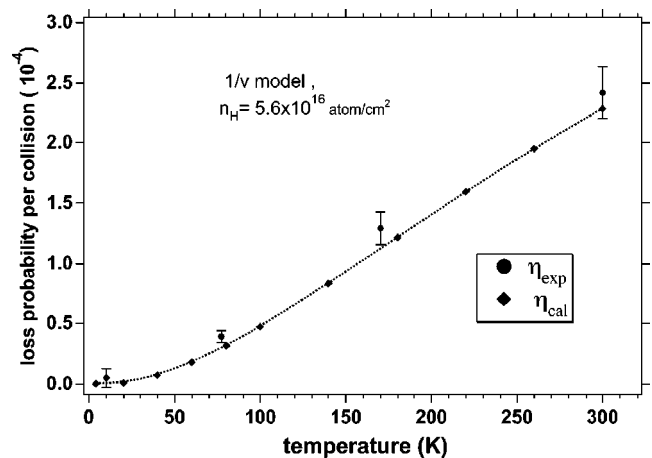


FIG. 7. Loss probability per collision calculated with $\sigma_{ie}(T)$ of ice and derived from experiment for the film model.

can be neglected. The absorption in Cu is temperature independent. Therefore, we can neglect interaction with the substrate and write the probability of the upscattering in the film as

$$\eta_{film} = \sigma_{ie}(E)N[2d + I(\lambda/d, E/V_F^f)], \quad (9)$$

where N is the volume density of hydrogen nuclei, d is the film thickness, λ is the UCN wavelength, $\sigma_{ie}(E)$ is the cross section of neutrons with energy $E=E_{UCN}-V_F^f$ in the film, and $I(\lambda/d, E/V_F^f)$ is an oscillating interference term. Since the latter must be averaged over the total surface with various λ/d , we can neglect it and use the formula

$$\eta_{film} = 2\sigma_{ie}(E)n, \quad (10)$$

where we replaced the term Nd by the surface density n . Thus, in this model the loss rate is independent of the incident angle and equal to $1/\tau = \eta_{film}\langle v \rangle$. As a result, η_{film} is larger than probability $\eta_{H,Cu}$ derived using the subbarrier model since here we do not have an additional factor f . Again, we see a quite good agreement between the calculated and experimental curves in Fig. 7.

V. SUMMARY

We reported a study of the temperature dependence of ultracold neutron upscattering carried out under ultrahigh-vacuum conditions and temperatures ranging down to 4 K. In addition to an oil-free pumping system, we used large-area cryopumping surfaces at both 77 K and 4 K to avoid cryoadsorption on the storage surface. Two states of the surface of the copper bottle were studied—after an ultrasonic wash in distilled water and after chemical cleaning and annealing + deuteration in heavy water vapor. Since the latter procedure made the surface hydrophobic and we carried out heating of the sample up to 450 K, we can attribute the T dependence to chemically bound hydrogen. The main observation of our experiment is a linearlike temperature dependence of the upscattering cross sections in the whole temperature range including the interval between 4 K and 77 K for both samples. For the deuterated surface the low-temperature measurement

was repeated twice. We did not see any differences in the data due to cooling or warming.

We analyzed our experimental data using an independent measurement of the surface hydrogen content (8%, $n=5.6 \times 10^{16} \text{ cm}^{-2}$), data from a prompt (n, γ) surface study, $\sigma_{ie}(300)=4-5.6 \text{ b}$, and phonon data (Cu, Cu-H, ice) from neutron scattering. Two basic models were considered, a dilute hydrogen solution in the metal lattice (H-Cu, subbarrier UCN interaction) and a hydrogenated film ($1/v$ law).

The information about the hydrogen surface density allowed us to estimate the contribution of both models to $\eta_{\text{expt}}(T)$ and to reliably rule out the model of subbarrier interaction. The absence of such data was a difficulty for all previous studies. Only the model of surface hydrogenated clusters or a film with low Fermi potential could explain the observed loss probability. In turn, the analysis of the low-temperature shape of $\eta_{\text{expt}}(T)$ and comparison of the calculated $\sigma_{ie}(300 \text{ K})$ with (n, γ) data allowed us to draw the conclusion that, again, it cannot be, film of the H-Cu compound but the hydrogen should be bound to a light atom like carbon or oxygen.

The latter conclusion was already drawn in our earlier presentation,⁴⁵ together with the assumption that C-H- or O-H-based molecules should have pronounced low-frequency vibrations. Since then we have analyzed available neutron scattering material about hydrogenated molecules. The intramolecular frequencies usually lie above 100 meV while intermolecular, i.e., translational and librational modes, are below 40 meV. The real issue was to satisfy several conditions simultaneously: a strong peak with energy $\leq 10 \text{ meV}$, a low weight and formula $X_a H_b$ with $b=2a$ to provide a negative potential, and probably $a \leq 2$ for the molecule to be light. For instance, low frequencies could easily be found in the heavy aromatic molecules⁴⁶ but then the amplitude of vibration is small due to the mass factor. The hydroxyl group OH commonly present on the surface together with oxides is known to have very high frequencies, about 100 meV. Another requirement would be a common presence on the surface in the form of clusters.

Finally, we succeed in finding a magic molecule. It turns out that the usual ice has a remarkably strong translational branch with a low-energy peak at 7 meV. The molecule is light, has negative Fermi potential, is commonly present on surfaces, and tends to adsorb preferably in hydrogen bound clusters.⁴⁷ The value of $\sigma_{ie}(300)=4 \text{ b}$ calculated using the experimental function $G_{ice}(\omega)$ of ice turns out to be in perfect agreement with the (n, γ) estimation and close to the experimental value $\sigma_{ie}(300)=7.2 \text{ b}$ of water. The loss probability $\eta_{ice}(T)$ calculated in the film model using the calculated ice cross sections and measured H density looks surprisingly similar to the experimental $\eta_{\text{expt}}(T)$. If the ice in the clusters is partly amorphous, then the frequencies will be washed out toward lower energies.⁴⁸ Thus, the presence of ice clusters, which could be reached by UCN's without intermediate barriers, could explain quite well both, the T dependence and the loss probability value.

It is easy to find the water before annealing but more difficult to explain the presence of the water afterward. A possibility would be that water clusters preferably grow at

the bottom of cracks or valleys between metal grains. A direct correlation between growths of both clusters of water and Cu_2O has been observed in Ref. 49. A very thin oxide film could seal the clusters and be transparent for UCN's.

Another possible but more exotic explanation would be H_2 bubbles as in the bulk of Cu. The first rotational state of the H_2 molecule has energy $\approx 15 \text{ meV}$.⁵⁰ Since the solubility of hydrogen is extremely low, the bulk hydrogen forms bubbles. The effect is well known in cryogenics. The density of the bulk hydrogen in our sample was found to be only 0.1% at depths below $1 \mu\text{m}$. One can imagine an increase of bubble density toward the surface. But then neutrons should penetrate through Cu walls thick enough to hold H_2 with a higher potential.

The waterlike layer as a possible cause of UCN upscattering was recently considered by Steyerl¹⁷ in connection with UCN storage on Fomblin oil with a probability of losses 5×10^{-4} per collision. He showed that reasonable concentration of H could explain the experimental data in the $1/v$ model, assuming a waterlike film covering the surface. The difficulty is that Fomblin oil is known to absorb the contamination into the bulk, the capability that provides excellent UCN storage properties even at room temperature when the Fomblin oil is cleaned by pumping. The situation looks similar to our problem of finding water clusters separated from the surface by a layer invisible for UCN's. Recent results and their analysis published in Ref. 8 allowed the authors to distinguish the surface effect from the bulk. Thus, the larger part of the room temperature losses were assigned to the surface. Theoretically, the latter was studied in Ref. 19 using experimental data about surface waves. The agreement is quite good. At low temperatures the surface effect becomes frozen and the bulk losses are in good agreement with the subbarrier calculation based on use of the inelastic cross section measured by transmission of 9 m/s neutrons. The effect of the bulk (coherent scattering) calculated for the pure polymer is much smaller than the experimental loss rate.⁵¹ The origin still has to be understood.

Nevertheless, it seems that at low temperatures it is only low-temperature Fomblin (LTF) and D_2O ice⁸ bulk effects where the subbarrier model of the UCN upscattering can be applied in agreement with experiment. On metals as we show in the present publication the film model is much more likely. This conclusion is in agreement with Be studies.^{25,26} Indeed, the two models have different dependences on the UCN energy which implies different shapes of the storage curve on a logarithmical scale vs linear storage time. The change in the loss rate due to upscattering (the difference between 6.5 K and 300 K) in Ref. 25 was 0.005 s^{-1} while the total loss rate at 4 K was 0.004 s^{-1} . This means that at 300 K the upscattering dominated. In the case of the valid subbarrier model the storage curve should be bent and look similar to the curve observed in a superthermal source²⁸ due to subbarrier absorption in the stainless steel. On the contrary, it looks linearlike which is in agreement with the film model. The temperature dependence was obviously deformed by the pinhole effect (different average energies at different temperatures) which complicate interpretation. It looks linear only up to 200 K but the 300 K point could be affected by pumping or by a phase transition. In the Gatchina

experiment the linearlike temperature dependence of the loss rate was observed down to 13 K at the very beginning before the trap was heated. The energy dependence measured in this experiment unfortunately was affected by an emptying procedure.²⁹ The result of the study by analysis with UCN's also indicates that UCN's are upscattered by a surface film with a cross section in the range 5–7 b independent of the material.²³

The surface of the Be is not so easy to oxidize as copper. It could also be a chemically bound amorphous hydrocarbon film with a different phonon spectrum and temperature dependence. The upscattering probability per collision in a Be-coated superthermal source at 77 K was very low, $\approx 6 \times 10^{-6}$, which is at the same level as a recent LTF lifetime measurement. Low-frequency excitations are known to be commonly present in amorphous matter but the relative contribution is not large in general.⁴⁸ To find the real cause of the low-temperature upscattering in different materials and work out a reliable quantitative model of UCN upscattering, we have to carry out an experimental study of samples with a known hydrogenated layer, use the (n, γ) technique to monitor the loss rate on hydrogen, and measure the cross section per proton. For instance, it could be a polymer film with a well studied spectrum of excitations. We would like to emphasize the need for *in situ* monitoring of the surface content by (n, γ) technique. Such measurement would be very helpful to study the origin of UCN upscattering in fluorinated polymers or other low-absorbing materials at low temperatures.

The theoretical technique used to calculate the total cross sections should also be tested further for the case of inelastic upscattering of ultracold neutrons. Our estimations was made using the first Born approximation. It works well for a wide range of neutron wavelengths down to cold (20 Å), whereas for energies comparable with the Fermi potential it is not valid in general.¹⁴ The corrections due to rescattering could increase the UCN sensitivity to low-frequency excitations and imply some special effects for the bulk and surface.⁵¹ The interesting question is interaction with clusters.

The development of a reliable theoretical description is of great importance to make progress in both ultracold neutron storage techniques and development of applications to solid state and surface studies using next generation UCN sources.² In the present work we have demonstrated a high sensitivity of the upscattering cross section to the lowest cutoff of the frequency and sensitivity to an inelastic signal

from a hydrogenated film ≈ 10 nm. This opens an interesting opportunity to use UCN's for unique studying of low-frequency excitations in the nanometer thick film with $V_F < E_{UCN}$ (polymers, deposited ice, and other gases) using both prompt γ analysis to monitor the hydrogen amount on the surface and measurement of the upscattering rate at different temperatures by the (n, γ) and storage techniques.

The study of $\sigma_{ie}(T)$ with UCN's is similar to the study of the temperature dependence in the specific heat measurement, but with hydrogen excitations and an emphasis on the thin surface layer ≈ 10 nm that is intermediate between the first monolayers, which are accessible to normal methods of surface physics, and true bulk matter. The anomalies found in the bulk C_V (for instance, the "boson" peak around 2–4 meV and the millikelvin anomaly in polymers) are still under intensive study by various modern methods. The lowest cutoff of the sensitivity of existing inelastic scattering instruments is restricted by the elastic peak. In our case an elastic reflection is invisible and we can detect the relative signal inelastic to elastic $\approx 10^{-6}$. At a reflectometer the background from the elastic reflection of the substrate would be a serious issue. Inelastic reflectometry simply does not exist at present while UCN's seem to be a natural tool for such a study. Another restriction lies in the thickness of the sample. The typical neutron inelastic scattering NIS sample thickness is of the order of 0.1–1 mm which means bulk samples. Nanoscale films could be studied only with electrons, which have sensitivity to other parameters than neutrons. The sensitivity to hydrogen with high-density UCN sources² could be as good as 10^{15} atoms/cm². The limitation would rather come from the ambient background.

ACKNOWLEDGMENTS

We would like to thank the TU Munich for support and the design and construction of the cryostat, the technical services of HMI and ILL, especially B. Urban (HMI) and T. Brenner, and the reactor division (ILL) for the excellent technical support during the experiment. The discussions with A. Steyerl and V. Morosov were especially fruitful and stimulating. We are very grateful to A. Kolesnikov (Argonne National Laboratory) for providing his phonon data about ice and detailed explanations. The work was supported by a program of bilateral cooperation between Russia and Germany, Grant No. RUS 02/030.

¹C. L. Morris, J. M. Anaya, T. J. Bowles, B. W. Filippone, P. Geltenbort, R. E. Hill, M. Hino, S. Hoedl, G. E. Hogan, T. M. Ito, T. Kawai, K. Kirch, S. K. Lamoreaux, C.-Y. Liu, M. Makela, L. J. Marek, J. W. Martin, R. N. Mortensen, A. Pichlmaier, A. Saunders, S. J. Seestrom, D. Smith, W. Teasdale, B. Tipton, M. Utsuro, A. R. Young, and J. Yuan, Phys. Rev. Lett. **89**, 272501 (2002).

²B. W. Wehring and A. R. Young, Trans. Am. Nucl. Soc. **84**, 120 (2000).

³E. Korobkina, R. Golub, B. W. Wehring, and A. R. Young, Phys. Lett. A **301**, 462 (2002).

⁴Y. Masuda, T. Kitagaki, K. Hatanaka, M. Higuchi, S. Ishimoto, Y. Kiyonagi, K. Morimoto, S. Mito, and M. Yoshimuro, Phys. Rev. Lett. **89**, 284801 (2002).

⁵P. R. Huffman, C. R. Brome, J. S. Butterworth, K. J. Coakley, M. S. Dewey, S. N. Dzhosyuk, R. Golub, G. L. Green, K. Habicht, S. K. Lamoreaux, C. E. Mattoni, D. N. McKinsey, F. E. Wietfeldt, and J. M. Doyle, Nature (London) **403**, 62 (2000).

- ⁶M. Cooper *et al.*, <http://p25ext.lanl.gov/edm/edm.html> (unpublished).
- ⁷V. E. Varlamov, V. V. Nesvizhevskii, A. P. Serebrov, R. R. Tal'daev, and A. G. Haritonov, *JETP* **87**, 426 (1998).
- ⁸S. S. Arzumanov, L. N. Bondarenko, V. I. Morozov, Yu. N. Panin, and P. Geltenbort, *Phys. At. Nucl.* **66**, 1820 (2003).
- ⁹V. V. Nesvizhevsky, *Phys. At. Nucl.* **65**, 400 (2002).
- ¹⁰V. K. Ignatovich and M. Utsuro, *Nucl. Instrum. Methods Phys. Res. A* **440**, 709 (2000).
- ¹¹S. Arzumanov, L. Bondarenko, S. Chernyavsky, W. Drexel, A. Fomin, P. Geltenbort, V. Morozov, Yu. Panin, J. Pendlebury, and K. Schreckenbach, *Phys. Lett. B* **483**, 15 (2000).
- ¹²S. S. Arzumanov, L. N. Bondarenko, E. I. Korobkina, V. I. Morozov, Yu. N. Panin, A. I. Fomin, S. M. Chernyavskii, S. V. Shilkin, P. Geltenbort, W. Drexel, J. Pendlebury, and K. Schreckenbach, *JETP Lett.* **65**, 690 (1997).
- ¹³S. S. Arzumanov, S. T. Belyev, L. N. Bondarenko, S. M. Ivanov, E. I. Korobkina, A. N. Lubimov, V. I. Morosov, A. I. Ryazanov, Yu. N. Panin, A. I. Fomin, S. M. Chernyavskii, P. Geltenbort, J. Pendlebury, and K. Schreckenbach, *JETP* **88**, 1 (1999).
- ¹⁴A. L. Barabanov and S. T. Belyaev, *Eur. Phys. J. B* **15**, 59 (2000).
- ¹⁵Yu. N. Pokotilovski, *Eur. Phys. J. B* **8**, 1 (1999).
- ¹⁶L. N. Bondarenko, P. Geltenbort, E. I. Korobkina, V. I. Morosov, and Yu. N. Panin, *Phys. At. Nucl.* **65**, 13 (2001).
- ¹⁷A. Steyerl, B. G. Erokolimsky, A. P. Serebrov, P. Geltenbort, N. Achiwa, Yu. N. Pokotilovsky, O. Kwon, M. S. Lasakov, I. A. Krasnoshchokova, and A. V. Vasilyev, *Eur. Phys. J. B* **28**, 299 (2002).
- ¹⁸A. P. Serebrov, J. Butterworth, M. Daum, A. K. Fomin, P. Geltenbort, K. Kirsh, I. A. Krasnoshchokova, M. S. Lasakov, Yu. P. Rudnev, V. E. Varlamov, and A. V. Vassiljev, *Phys. Lett. A* **309**, 218 (2003).
- ¹⁹S. K. Lamoreaux and R. Golub, *Phys. Rev. C* **66**, 044309 (2002).
- ²⁰E. V. Lychagin, D. G. Kartashov, A. Yu. Muzychka, V. V. Nesvizhevsky, G. V. Nekhaev, and A. V. Strelkov, *Phys. At. Nucl.* **65**, 1995 (2002).
- ²¹A. Serebrov, V. Varlamov, P. Geltenbort, A. Kharitonov, R. Tal'daev, I. Krasnoschekova, A. Vassiljev, O. Zherebtsov, M. Daum, R. Henneck, K. Kirsh, J. Butterworth, and K. Schreckenbach, UCN workshop, PNPI, Gatchina, 2003, http://nrd.pnpi.spb.ru/UCN_CNS (unpublished).
- ²²L. Bondarenko, S. Chrnayvsky, A. Fomin, P. Geltenbort, V. Morozov, and S. Shilkin, *Physica B* **234-236**, 1189 (1997).
- ²³L. N. Bondarenko, Third UCN Workshop, PNPI, Gatchina, 2001, <http://nrd.pnpi.spb.ru/SEREBROV/3rd/talks/talks.htm> (unpublished).
- ²⁴W. A. Lanford and R. Golub, *Phys. Rev. Lett.* **39**, 1509 (1977).
- ²⁵P. Ageron, W. Mampe, and A. I. Kilvington, *Z. Phys. B: Condens. Matter* **59**, 261 (1985).
- ²⁶A. G. Kharitonov, V. V. Nesvizhevsky, A. P. Serebrov, R. R. Tal'daev, V. E. Varlamov, A. V. Vasilyev, V. P. Alfimankov, V. I. Luschnikov, V. N. Shvetsov, and A. V. Strelkov, *Nucl. Instrum. Methods Phys. Res. A* **284**, 98 (1989).
- ²⁷S. Arzoumanov *et al.*, ILL Experimental reports 2001, Experiment 3-14-121, www.ill.fr (unpublished).
- ²⁸R. Golub, C. Jewell, P. Ageron, W. Mampe, B. Heckel, and I. Kilvington, *Z. Phys. B: Condens. Matter* **51**, 187 (1983).
- ²⁹V. V. Nesvizhevskii, A. P. Serebrov, R. R. Tal'daev, A. G. Kharitonov, V. P. Alfimankov, A. V. Strelkov, and V. N. Shvetsov, *Sov. Phys. JETP* **75**, 405 (1992).
- ³⁰V. E. Varlamov, V. V. Nesvizhevskiy, A. P. Serebrov, R. R. Tal'daev, A. G. Kharitonov, P. Geltenbort, Ts. Ts. Pantelev, A. V. Strelkov, V. N. Schvetsov, M. Pendlebury, and K. Schreckenbach, *JETP* **87**, 426 (1998).
- ³¹S. S. Arzumanov, L. N. Bondarenko, V. I. Morozov, Yu. Panin, and P. Geltenbort, *Phys. At. Nucl.* **66**, 1820 (2003).
- ³²A. Steyerl, UCN Workshop, PNPI, Gathina, 2003, http://nrd.pnpi.spb.ru/UCN_CNS (unpublished).
- ³³Yu. N. Pokotilovski, *Nucl. Instrum. Methods Phys. Res. A* **425**, 320 (1999); Yu. N. Pokotilovski, *JETP* **96**, 172 (2003).
- ³⁴D. I. Blochintzev and N. M. Plakida, *Phys. Status Solidi B* **82**, 627 (1977).
- ³⁵V. K. Ignatovich, *Physics of Ultracold Neutrons* (Clarendon Press, Oxford, 1990), Chap. 6, pp. 174, 216.
- ³⁶L. Bondarenko, S. Chrnayvsky, A. Fomin, P. Geltenbort, V. Morozov, and S. Shilkin, *Physica B* **234-236**, 1189 (1997).
- ³⁷L. N. Bondarenko, Third UCN Workshop, PNPI, Gatchina, 2001, <http://nrd.pnpi.spb.ru/SEREBROV/3rd/talks/talks.htm> (unpublished).
- ³⁸V. F. Turchin, *Slow Neutrons* (Sivan Press, Jerusalem, 1967), p. 45.
- ³⁹E. C. Svensson, B. N. Blockhouse, and J. M. Rowe, *Phys. Rev.* **155**, 619 (1967).
- ⁴⁰A. I. Kolesnikov, V. E. Antonov, A. M. Balagurov, S. Bennington, and M. Prager, *J. Phys.: Condens. Matter* **6**, 9001 (1994).
- ⁴¹R. Weinstock, *Phys. Rev.* **65**, 1 (1944).
- ⁴²S. Arzumanov, L. Bondarenko, P. Geltenbort, E. Korobkina, V. Morozov, Yu. Panin, A. Fomin, and S. Chernjavsky, *Nucl. Instrum. Methods Phys. Res. A* **440**, 690 (2000).
- ⁴³A. I. Kolesnikov, E. G. Ponyatovsky, I. Natkaniec, and L. S. Smirnov, *J. Phys.: Condens. Matter* **6**, 375 (1994).
- ⁴⁴A. I. Kolesnikov and J.-C. Li, *Physica B* **234-236**, 34 (1997).
- ⁴⁵S. Arzumanov, J. Butterworth, R. Golub, P. Geltenbort, and E. Korobkina, Report No. ISINN-10, JINR, Dubna, Russia (2002), p. 349.
- ⁴⁶P. A. Reynolds, *J. Chem. Phys.* **56**, 2928 (1972).
- ⁴⁷P. A. Thiel, F. M. Hoffmann, and W. H. Weinberg, *J. Chem. Phys.* **75**, 5556 (1981); D. Lackey, J. Schott, B. S. Staehler, and J. K. Sass, *J. Chem. Phys.* **91**, 1365 (1989).
- ⁴⁸A. I. Kolesnikov, Jichen Li, S. F. Parker, R. S. Eccleston, and C.-K. Loong, *Phys. Rev. B* **59**, 3569 (1999).
- ⁴⁹T. Aastrup, Ph.D. thesis, Royal Institute of Technology, Stockholm, Sweden, 1999.
- ⁵⁰C. M. Brown, *Chem. Phys. Lett.* **329**, 311 (2000).
- ⁵¹A. N. Barabanov and S. T. Belyev (unpublished).